

Fast adsorption of methylene blue on polyacrylic acid-bound iron oxide magnetic nanoparticles

Sou-Yee Mak, Dong-Hwang Chen*

Department of Chemical Engineering, National Cheng Kung University, Tainan, Taiwan 701

Received 12 June 2003; received in revised form 23 July 2003; accepted 7 October 2003

Abstract

The adsorption of methylene blue (MB) from an aqueous solution by polyacrylic acid-bound iron oxide magnetic nanoparticles was studied. It was shown that the novel magnetic nano-adsorbent was quite efficient for the adsorption/desorption of MB. In the aqueous solution of MB at 25 °C, the adsorption data could be fitted by the Langmuir equation with a maximum adsorption amount of 0.199 mg/mg and a Langmuir adsorption equilibrium constant of 10.1 ml/mg. The adsorption capacity increased with the increase in solution pH (2–10) and the adsorption process was endothermic in nature with an enthalpy change (ΔH) of 30.9 kJ/mol at 10–40 °C. By using the methanol solution of acetic acid, the adsorbed MB could be desorbed. In addition, it was notable that both the adsorption and desorption of MB were quite fast and could be completed within 2 min due to the absence of internal diffusion resistance.

© 2003 Elsevier Ltd. All rights reserved.

Keywords: Adsorption; Iron oxide; Polyacrylic acid; Methylene blue; Magnetic nanoparticles

1. Introduction

Effluents from the textile industries are important sources of water pollution, because dyes in wastewater undergo chemical as well as biological changes, consume dissolved oxygen, and destroy aquatic life. Moreover, some dyes and their degradation products may be carcinogens and toxic. Therefore, it is necessary to treat textile effluents prior to their discharge into the receiving water.

Adsorption is a conventional but efficient technique to remove dyes from aqueous solutions.

Many kinds of adsorbents for various applications have been commercialized or are developing [1–9]. In general, these adsorbents are highly porous particles in order to ensure adequate surface area for adsorption. However, the existence of intraparticle diffusion may lead to the decreases in the adsorption rate and available capacity, particularly for macromolecules. Therefore, to develop an adsorbent with large surface area and small diffusion resistance has significant importance in practical use [10].

Magnetic nanoparticles have great applications in the fields of high-density data storage, ferrofluids, magnetic resonance imaging, wastewater treatment, bioseparation, and biomedicine [11–17]. They meet the above requirements and can be

* Corresponding author. Tel.: +886-6-2757575x62680; fax: +886-6-2344496.

E-mail address: chendh@mail.ncku.edu.tw (D.-H. Chen).

easily recovered or manipulated with an external magnetic field. Numerous types of magnetic nanoparticles for various applications could be tailored by using functionalized natural or synthetic polymers to impart surface reactivity [12,17–19].

Recently, we developed a novel magnetic nano-adsorbent using iron oxide nanoparticles as cores and polyacrylic acid (PAA) as ionic exchange groups [18]. It possessed a high ion-exchange capacity and was quite effective for the enzyme recovery. In this work, the PAA-bound iron oxide magnetic nanoparticles were further used for the removal of a basic dye methylene blue (MB). The influences of experimental conditions such as MB concentration, pH, temperature, ionic strength and desorption solution were investigated to obtain information on treating effluents from the dye industry.

2. Experimental

2.1. Chemicals

Methylene blue (Basic blue 9; CI-52015) was obtained from Kasei Kogyo Co. (Tokyo). Carbodiimide was supplied by Sigma Chemical Co. (St. Louis, MO). Polyacrylic acid solution (25%, degree of polymerization = 2000–3000) was purchased from Showa Chemical Co. (Tokyo). Ferric chlorides, 6-hydrate and ferrous chloride tetrahydrate were the products of J.T. Baker (Phillipsburg) and Fluka (Buchs), respectively. Ammonium hydroxide (29.6%) was supplied by TEDIA (Fairfield). The water used throughout this work was the reagent-grade water produced by Milli-Q SP ultra-pure-water purification system of Nihon Millipore Ltd., Tokyo. All other chemicals were the guaranteed or analytic grade reagents commercially available and used without further purification.

2.2. Preparation of PAA-bound iron oxide magnetic nanoparticles

PAA-bound iron oxide magnetic nanoparticles were prepared according to our previous works [18]. Iron oxide nanoparticles were prepared by

co-precipitating Fe^{2+} and Fe^{3+} ions by ammonia solution and treating under hydrothermal conditions. The ferric and ferrous chlorides (molar ratio 2:1) were dissolved in water at a concentration of 0.3 M iron ions. Chemical precipitation was achieved at 25 °C under vigorous stirring by adding NH_4OH solution (29.6%). During the reaction process, the pH was maintained at about 10. The precipitates were heated at 80 °C for 30 min, then washed several times with deionized water and ethanol, and finally dried in a vacuum oven at 70 °C.

For the binding of PAA, 100 mg of iron oxide nanoparticles were first added to 2 ml of buffer A (0.003 M phosphate, pH 6). Then, the reaction mixture was sonicated for 10 min after adding 0.5 ml of carbodiimide solution (0.025 g/ml in buffer A). Finally, 2.5 ml of PAA solution (60 mg/ml in buffer A) were added and the reaction mixture was sonicated for 30 min. The binding process was carried out at a constant temperature of 4 °C. The PAA-bound iron oxide nanoparticles were recovered from the reaction mixture by placing the bottle on a permanent magnet with a surface magnetization of 6000 gauss. They settled within 1–2 min and then were washed with deionized water.

2.3. Characterization

The size of iron oxide nanoparticles was observed by transmission electron microscopy (TEM) using a Jeol Model JEM-1200EX at 80 kV. The magnetic measurement was done using a superconducting quantum interference device (SQUID) magnetometer (MPMS7, Quantum Design). The amount of PAA bound on iron oxide nanoparticles was estimated by the percentage weight losses from the thermogravimetric analysis (TGA) done on the dried magnetic nanoparticles in air with a heating rate of 10 °C/min on the Shimadzu TA-50WSI TGA. The ion exchange capacity of PAA-bound iron oxide magnetic nanoparticles was determined as follows. First, 112 mg of nanoparticles was incubated in 5 ml of 1.0 M NaCl. The preliminary experiment revealed the adsorption process reached equilibrium after mixing by vortex for about 1 min, the nanoparticles were recovered magnetically after several minutes and then rinsed with water. Secondary,

the nanoparticles were added to 5 ml of HNO_3 solution (pH 3) to release the Na^+ ions. After mixing by vortex for several minutes, the mixture was separated magnetically and the supernatant was used to determine the concentration of Na^+ ions by inductively coupled plasma atomic emission spectrometry (Jobin Yvon PA Norama).

2.4. Adsorption and desorption studies

The adsorption of MB onto the PAA-bound iron oxide magnetic nanoparticles was carried out in 0.03 M phosphate buffer at 25 °C and pH 9. In general, 112 mg nanoparticles were added to 5 ml of MB solution (0.5–8.0 mg/ml). After mixing by vortex for 2 min, nanoparticles were removed magnetically from MB solution. The adsorption amounts of MB were estimated from the concentration change of MB in solution after adsorption by the spectrophotometric method at 664 nm (Hitachi U-3000 UV/vis spectrophotometer).

Desorption of MB was performed by putting the removed nanoparticles into methanol solution containing 2–12% acetic acid [13]. After mixing for several minutes and removing the nanoparticles, the concentration of MB in liquid solution was measured to estimate the amount of MB desorbed.

3. Results and discussion

3.1. Characteristics of PAA-bound iron oxide magnetic nanoparticles

From the TEM analysis, the resultant PAA-bound iron oxide nanoparticles were found to be very fine. Their mean diameter was 12 nm. The magnetic measurement indicated that they were superparamagnetic with a saturation magnetization of 62 emu/g at 25 °C. The TGA curve for the PAA-bound iron oxide nanoparticles showed a sharp weight loss of about 10.7% around 260 °C due to the burning of PAA, and remained unchanged from 260 to 400 °C because only iron oxide existed within the temperature range. Thus, the weight ratio of bound PAA to Fe_3O_4 could be calculated to be 0.12. Since the density of Fe_3O_4

(5.18 g/ml) and the average molecular weight of PAA (180,000), it was estimated that averagely two PAA molecules were bound to each Fe_3O_4 nanoparticle.

3.2. Effect of pH

The effect of pH on the adsorption of MB (2.0 mg/ml) by the PAA-bound iron oxide magnetic nanoparticles (22.4 mg/ml) in 0.03 M phosphate buffer at 25 °C was illustrated in Fig. 1. It was found that the adsorption capacity of MB increased with increasing the solution pH [3,6,7]. This could be attributed to the fact that the protonation of carbonyl groups of PAA became insignificant at high pH. Since the adsorption amount of MB remained constant at pH 7–10, the following studies were conducted at a fixed pH of 9.

It was noteworthy that the adsorption of MB reached equilibrium within about 2 min. Such a fast adsorption rate could be referred to the absence of internal diffusion resistance.

3.3. Adsorption isotherm

The equilibrium isotherm of MB adsorption by the PAA-bound iron oxide magnetic nanoparticles (22.4 mg/ml) in 0.03 M phosphate at pH 9 and 25 °C is shown in Fig. 2. The adsorption behavior could be described by the Langmuir adsorption equation [3].

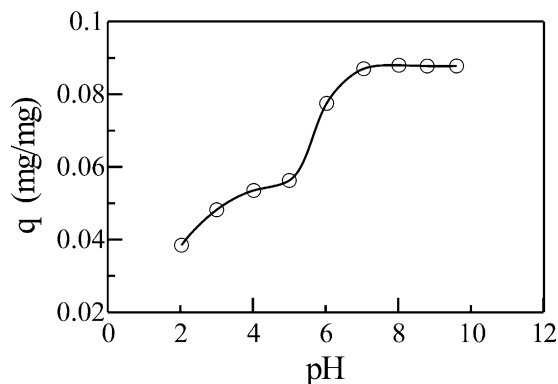


Fig. 1. Adsorption of MB on PAA-bound iron oxide nanoparticles as a function of pH. Conditions: (PAA-bound iron oxide nanoparticles: 22.4 mg/ml; MB: 2.0 mg/ml; phosphate: 0.03 M; temperature: 25 °C).

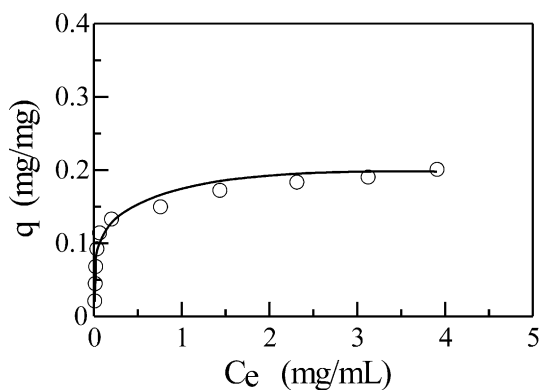


Fig. 2. Adsorption isotherm of MB on PAA-bound iron oxide nanoparticles. Conditions: (PAA-bound iron oxide nanoparticles: 22.4 mg/ml; MB: 0.5–8.0 mg/ml; phosphate: 0.03 M; temperature: 25 °C; pH: 9).

$$\frac{C_e}{q} = \frac{1}{Kq_m} + \frac{C_e}{q_m} \quad (1)$$

where q is the equilibrium adsorption amount of MB (mg/mg), C_e is the equilibrium MB concentration in solution (mg/ml), q_m is the maximum adsorption amount of MB per mg of adsorbent (mg/mg) and K is the Langmuir adsorption equilibrium constant (ml/mg). As shown in Fig. 3, the plot of C_e/q vs. C_e yielded a straight line. From the slope and intercept, the values of q_m and K might be estimated to be 0.199 mg/mg and 10.1 ml/mg, respectively.

3.4. Effect of temperature

The effect of temperature on the adsorption of MB (4.0 mg/ml) by the PAA-bound iron oxide nanoparticles (22.4 mg/ml) in 0.03 M phosphate buffer at pH 9 was indicated in Fig. 4. The adsorption amount of MB increased with increasing temperature. The plot of $\log(q/C_e)$ vs. $1/T$ was indicated in Fig. 5. From the slope ($-\Delta H/2.303R$), the change of enthalpy (ΔH) at 10–40 °C could be determined to be 30.9 kJ/mol. This value was comparable with the other adsorbents [6,7], and revealed the adsorption process was endothermic in nature.

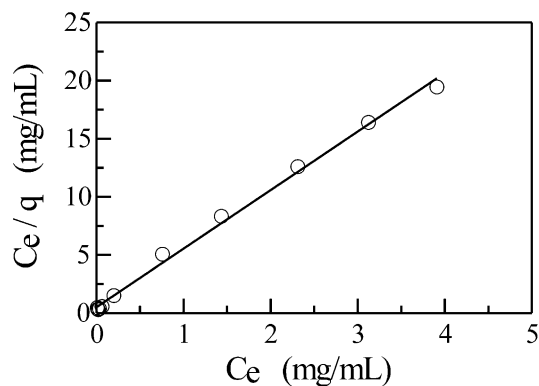


Fig. 3. A plot of C_e/q against C_e for the adsorption of MB on PAA-bound iron oxide nanoparticles. Conditions: (PAA-bound iron oxide nanoparticles: 22.4 mg/ml; MB: 0.5–8.0 mg/ml; phosphate: 0.03 M; temperature: 25 °C; pH: 9).

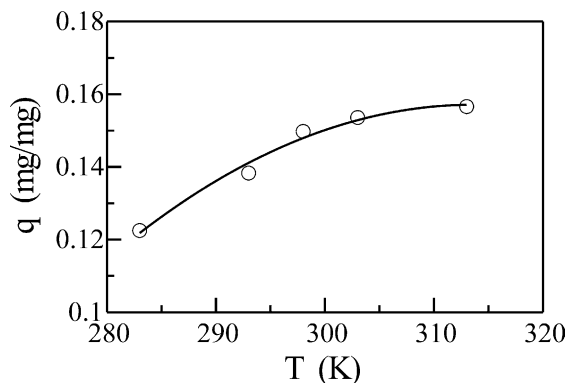


Fig. 4. Adsorption of MB on PAA-bound iron oxide nanoparticles as a function of temperature. Conditions: (PAA-bound iron oxide nanoparticles: 22.4 mg/ml; MB: 4.0 mg/ml; phosphate: 0.03 M; pH: 9).

3.5. Effect of ionic strength

The effect of ionic strength on the adsorption of MB (5.0 mg/ml) by the PAA-bound iron oxide nanoparticles (22.4 mg/ml) was examined in KCl-containing phosphate buffer (0.03 M, pH 9). The result was shown in Fig. 6. It was found that the adsorption amount of MB remained almost constant with the increase of KCl concentration up to 50 mM. This implied that the electrostatic attraction between the negatively charged PAA molecules on the iron oxide nanoparticles and the positively charged MB molecules was not affected significantly by KCl under the examined condi-

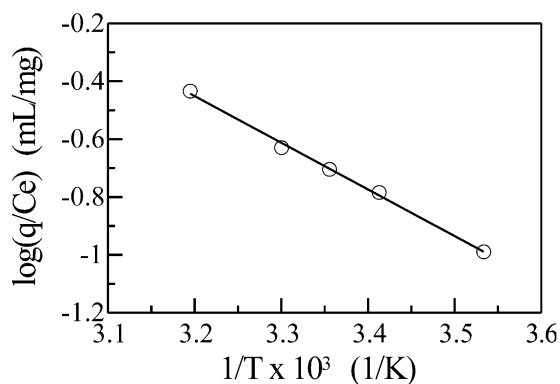


Fig. 5. A plot of $\log(q/C_e)$ against $1/T$. Conditions: (PAA-bound iron oxide nanoparticles: 22.4 mg/ml; MB: 4.0 mg/ml; phosphate: 0.03 M; pH: 9).

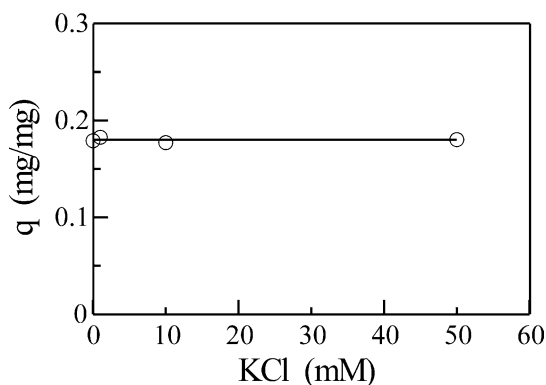


Fig. 6. Adsorption of MB on PAA-bound iron oxide nanoparticles as a function of KCl concentration. Conditions: (PAA-bound iron oxide nanoparticles: 22.4 mg/ml; MB: 5.0 mg/ml; phosphate: 0.03 M; temperature: 25 °C; pH: 9).

tion. The effect of KCl concentration above 50 mM was not examined because MB could not be dissolved completely.

3.6. Desorption

The desorption of MB might be achieved using a methanol solution of acetic acid [13]. As shown in Fig. 7, the percentage of MB desorbed increased with increasing the content of acetic acid. When the content of acetic acid in methanol solution was increased up to 4%, about 80% of MB could be

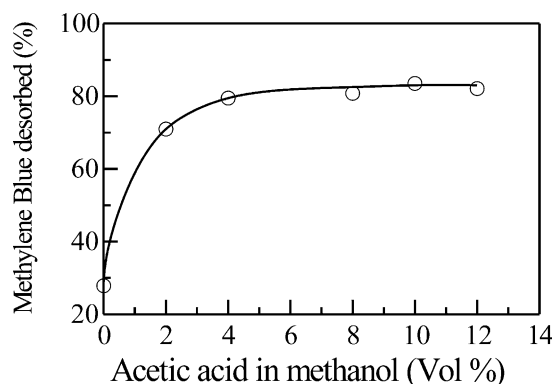


Fig. 7. Desorption of MB from PAA-bound iron oxide nanoparticles as a function of acetic acid concentration in methanol. Adsorption conditions: (PAA-bound iron oxide nanoparticles: 22.4 mg/ml; MB: 2.0 mg/ml; phosphate: 0.03 M; temperature: 25 °C; pH 9). Desorption conditions: (PAA-bound iron oxide nanoparticles: 22.4 mg/ml; temperature: 25 °C).

desorbed. By multiple desorption (about 3 steps), MB could be completely desorbed.

Noteworthy, the desorption equilibrium of MB was achieved within about 2 min, similar to the adsorption equilibrium. This also could be attributed to the absence of internal diffusion resistance.

4. Conclusion

MB could be recovered fast and efficiently from an aqueous solution by the PAA-bound iron oxide magnetic nanoparticles due to large specific surface area and the absence of internal diffusion resistance. The adsorption behavior could be described by Langmuir isotherm, and the adsorption amount of MB increased with both the increases in solution pH and temperature. The adsorbed MB could be desorbed using the acetic acid-containing methanol solution. Both the adsorption and desorption of MB reached equilibrium within 2 min.

References

- [1] Ruthven DM. Principles of adsorption and adsorption processes. New York: John Wiley & Sons; 1984.

- [2] McKay G. Use of Adsorbents for the removal of pollutants from wastewaters. CRC Press: Boca Raton; 1995.
- [3] Kannan N, Sundaram MM. Kinetics and mechanism of removal of methylene blue by adsorption on various carbons—a comparative study. *Dyes and Pigments* 2001; 51(1):25–40.
- [4] Yu Y, Zhuang YY, Wang ZH. Adsorption of water-soluble dye onto functionalized resin. *J Colloid Interface Sci* 2001;242(2):288–93.
- [5] Hirata M, Kawasaki N, Nakamura T, Matsumoto K, Kabayama M, Tamura T, et al. Adsorption of dyes onto carbonaceous materials produced from coffee grounds by microwave treatment. *J Colloid Interface Sci* 2002;254(1): 17–22.
- [6] Ghosh D, Bhattacharyya KG. Adsorption of methylene blue on kaolinite. *Appl Clay Sci* 2002;20(6):295–300.
- [7] Lee CK, Low KS, Chung LC. Removal of some organic dyes by hexane-extracted spent bleaching earth. *J Chem Tech Biotechnol* 1997;69(1):93–9.
- [8] Delval F, Crini G, Morin N, Vebrel J, Bertini S, Torri G. The sorption of several types of dye on crosslinked polysaccharides derivatives. *Dyes and Pigments* 2002;53(1):79–92.
- [9] Robinson T, Chandran B, Nigam P. Removal of dyes from a synthetic textile dye effluent by biosorption on apple pomace and wheat straw. *Water Res* 2002;36(11): 2824–30.
- [10] Dabrowski A, Bülow M, Podkościelny P. In: Dekany I, editor. *Adsorption and Nanostructures*. Berlin, Heidelberg: Springer-Verlag; 2002. p. 70–5.
- [11] Sun S, Murray CB, Weller D, Folks L, Moser A. Monodisperse FePt nanoparticles and ferromagnetic FePt nanocrystal superlattices. *Science* 2000;287:1989–92.
- [12] Pieters BR, Williams RA, Webb C. In: Williams RA, editor. *Colloid and surface engineering: applications in the process industries*. Oxford: Butterworth-Heinemann; 1992. p. 248–86.
- [13] Šafařík I. Removal of organic polycyclic compounds from water solutions with a magnetic chitosan based sorbent bearing copper phthalocyanine dye. *Water Res* 1995;29(1): 101–5.
- [14] Denizli A, Say R. Preparation of magnetic dye affinity adsorbent and its use in the removal of aluminium ions. *J Biomater Sci Polym Edn* 2001;12(10):1059–73.
- [15] Schütt W, Grüttner C, Häfeli U, Zborowski M, Teller J, Putzar H, et al. Applications of magnetic targeting in diagnosis and therapy—possibilities and limitation: a mini—review. *Hybridoma* 1997;16(1):109–17.
- [16] Häfeli U, Schütt W, Teller J, Zborowski M. *Scientific and clinical applications of magnetic carriers*. New York: Plenum Press; 1997.
- [17] Xu Z, Liu Q, Finch JA. In: Schwarz JA, Contescu CI, editors. *Surfaces of nanoparticles and porous materials*. New York: Marcel Dekker; 1999. p. 31–50.
- [18] Liao MH, Chen DH. Preparation and characterization of a novel magnetic nano-adsorbent. *J Mater Chem* 2002; 12(12):3654–9.
- [19] Chen DH, Liao MH. Preparation and characterization of YADH-bound magnetic nanoparticles. *J Mol Catal B-Enzymatic* 2002;16(5-6):283–91.